

Multi-scale wireless sensor node for health monitoring of civil infrastructure and mechanical systems

Stuart G. Taylor^{1,2} Kevin M. Farinholt¹, Gyuhae Park^{1*}, Michael D. Todd²
and Charles R. Farrar¹

¹The Engineering Institute, Los Alamos National Laboratory, NM 87545, USA

²Department of Structural Engineering, University of California, San Diego, CA 92093, USA

(Received October 14, 2009, Accepted February 20, 2010)

Abstract. This paper presents recent developments in an extremely compact, wireless impedance sensor node (the WID3, Wireless Impedance Device) for use in high-frequency impedance-based structural health monitoring (SHM), sensor diagnostics and validation, and low-frequency (< ~1 kHz) vibration data acquisition. The WID3 is equipped with an impedance chip that can resolve measurements up to 100 kHz, a frequency range ideal for many SHM applications. An integrated set of multiplexers allows the end user to monitor seven piezoelectric sensors from a single sensor node. The WID3 combines on-board processing using a microcontroller, data storage using flash memory, wireless communications capabilities, and a series of internal and external triggering options into a single package to realize a truly comprehensive, self-contained wireless active-sensor node for SHM applications. Furthermore, we recently extended the capability of this device by implementing low-frequency analog-to-digital and digital-to-analog converters so that the same device can measure structural vibration data. The compact sensor node collects relatively low-frequency acceleration measurements to estimate natural frequencies and operational deflection shapes, as well as relatively high-frequency impedance measurements to detect structural damage. Experimental results with application to SHM, sensor diagnostics and low-frequency vibration data acquisition are presented.

Keywords: structural health monitoring; impedance method; piezoelectric active-sensors; sensor diagnostics; wireless hardware.

1. Introduction

Structural health monitoring (SHM) is the process of detecting damage in structures. The goal of SHM is to improve the safety and reliability of aerospace, civil and mechanical infrastructure by detecting damage before it reaches a critical state. To achieve this goal, technology is being developed to replace qualitative visual inspection and time-based maintenance procedures with more quantifiable and automated damage assessment processes. These processes are implemented using both hardware and software with the intent of achieving more cost-effective condition-based maintenance. A more detailed general discussion of SHM can be found in Worden and Dulieu-Barton (2004).

The implementation of SHM is an integrated paradigm of networked sensing and actuation, data interrogation (signal processing and feature extraction), and statistical assessment (classification of

*Corresponding Author, Technical Staff Member, E-mail: gpark@lanl.gov

damage existence, location and/or type) that treats structural health assessments in a systematic way. An appropriate sensor network is always required as a first line of attack in observing the structural system behavior in such a way that suitable signal processing and damage-sensitive feature extraction on the measured data may be performed efficiently.

A specific topic that has not been extensively addressed in the SHM literature is the development of rigorous approaches to designing the data acquisition portion of SHM sensing system. To date, almost all such system designs are done somewhat in an *ad hoc* manner where the engineer picks a sensing system that is readily available and with which they are familiar, and then attempts to demonstrate that a specific type of damage can be detected with that system. In many cases, this approach has been shown to be ineffective. As a result, researchers have begun to develop sensor networks suited for SHM objectives. Because the cost of implementing a vast network of sensors using traditional wired systems can become prohibitively high, there has been a recent shift toward the use of wireless sensor nodes, which are well-summarized by Spencer *et al.* (2004) and Lynch and Loh (2006). Advances in wireless communications and low power electronics have enabled the development of power efficient, compact sensor nodes for SHM and other engineering applications.

This paper presents an overview of a wireless sensor node specifically designed for structural health monitoring and sensor diagnostics in both a relatively high frequency regime, wherein the impedance method is typically used, as well as a relatively low-frequency regime, wherein traditional sensing methods such as modal analysis and time-domain identification methods are used.

2. Hardware design and capabilities

The wireless impedance device (WID) was originally developed based on capabilities demonstrated in previous studies of the impedance-based structural health monitoring method (Park *et al.* 2003, Park *et al.* 2006c, Bhalla and Soh 2004, Giurgiutiu *et al.* 2004). The basic concept of the impedance method is to use high-frequency (tens to hundreds of kHz) vibrations to monitor the local area of a structure for changes in structural impedance that would indicate damage or imminent damage. This process is possible using piezoelectric sensor/actuators whose electrical impedance is directly related to the structure's mechanical impedance through bonding. This electromechanical coupling is exploited to detect how changing mechanical system parameters that may correlate with damage, such as resonant frequencies or modal damping, reflect in measureable voltage potentials in the bonded sensor. Another critical aspect of the impedance method is that it can be implemented with relatively low power, compared to other active-sensing SHM techniques such as Lamb wave-based methods. The hardware required for implementing Lamb wave propagations needs much higher sampling rates and higher peak-power capabilities, compared to that of impedance methods. The impedance method also has applications in sensor self-diagnostics in determining the operational status of piezoelectric active-sensors used in SHM (Park *et al.* 2006a, 2006b, Park *et al.* 2009b, Overly *et al.* 2009).

In the past, several research efforts have focused on the development of wireless sensor nodes that capitalize on the capability of the impedance method. Grisso and Inman (2008) developed a stand-alone prototype of active-sensing unit, incorporating impedance data acquisition, local-computation, wireless communication of the results and a renewable power supply via several different types of energy harvesting techniques. This prototype has been substantially improved by Kim *et al.* (2009) and Zhou *et al.* (2009). This new prototype eliminates the use of a digital-to-analog converter which

requires a large memory space and power consumption, allowing for extremely low-power operation (<18 mW). Wang and You (2008) also introduced a new circuit implementation for electrical impedance monitoring coupled with the use of wireless telemetry.

The core component of WID is the Analog Devices AD5933 impedance chip, which is capable of resolving impedance measurements up to 100 kHz. The use of AD5933 for measuring impedance signatures for SHM is firstly proposed by the authors (Mascarenas *et al.* 2006), and substantially investigated producing several versions of snap-on hardware with experimental validation. (Mascarenas *et al.* 2007, Overly *et al.* 2008, Taylor *et al.* 2009). By following the similar concept, several different prototypes were also produced by other researchers using the AD5933 chip (Park *et al.* 2009a, Kim *et al.* 2010).

The first generations of the WID, the WID 1.5 and 2.0, developed by our research team (Mascarenas *et al.* 2007, Overly *et al.* 2008) are shown in Fig. 1 (left), along with the current version WID 3.0. The WID 2.0 was developed to address some of the limitations of the WID 1.5, including the ability to monitor only a single active-sensor, limited triggering capabilities, and the high power demands of the wireless telemetry components. The WID 3.0 provides further increased capabilities over the previous generations, with advanced communication capabilities, increased triggering options, more data storage capabilities, as well as multiple power options coupled with a power conditioning component that allows the use with a variety of energy harvesting options. The WID 3.0 can self-configure into a network with neighboring sensor nodes at fixed time intervals or in the presence of a ‘mobile host’ that is brought in to interrogate the sensor network. The WID 3.0 has been designed to operate using multiple power options, including the ability to store energy harvested from the environment and/or energy received through radio frequency (RF) energy transmission.

In addition to improving the capabilities and functionality of the previous WID versions, the WID 3.0 has been designed to function as part of a modular hardware platform that incorporates other sensing capabilities on separate boards, such as time-domain measurement capabilities. By combining modules, resources such as the telemetry, processing, data storage and respective measurement capabilities of each module may be shared, resulting in a highly functional sensor node. One such configuration is shown in Fig. 1 (right), where the WID3 has been combined with the Wireless Data Acquisition (WiDAQ) board. This integrated sensor node combines both actuation and sensing capabilities into a single package with the ability to implement multiple SHM techniques for the rapid health assessment of civil, aerospace and mechanical infrastructure.

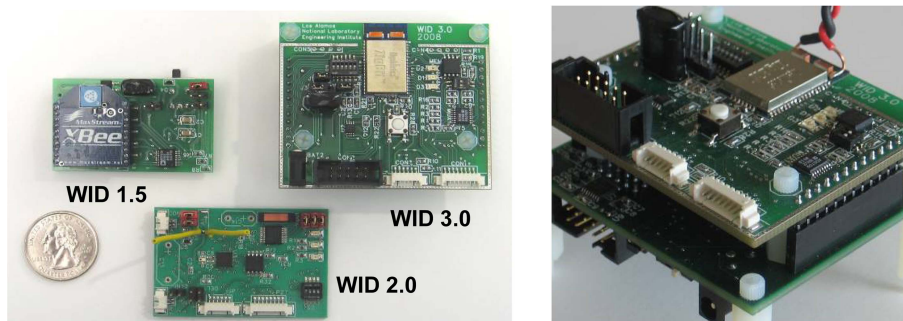


Fig. 1 Three generations of wireless impedance devices (shown left) and the combined WID3/WiDAQ module (shown right)

2.1 WID 3.0 hardware and capabilities

The major hardware components of the WID 3.0 are shown in Fig. 2. Like the previous generations, the WID 3.0 is controlled by an ATmega1281v microcontroller. The WID 3.0 uses a ZigBit module which integrates the ATmega1281v microprocessor with Atmel’s AT86RF230 transceiver module within a single compact package. The microcontroller itself is manufactured by Atmel and is part of their 8-bit AVR line. This microcontroller contains 128 kB of program memory allowing for complex and robust algorithms to be loaded on the chip. It also contains 8 kB of memory for computational requirements. The ATmega1281 comes from a line of microprocessors that have available to them a large open source development community. Atmel is developing future versions with enhanced capabilities, which include more memory and EEPROM, while maintaining the same form factor that would allow for pin compatibility. These features would help with applications and expansion of capabilities in future versions of the WID. The wireless data transmission solution is also produced by Atmel and integrated within the ZigBit module. This solution is an 802.15.4 compliant radio, which uses an open MAC protocol distributed by ZigBit. The availability of the MAC table facilitates programming to the wireless standard for robust data transmission. The AT86RF230 has very low energy requirements and low external component counts, making it particularly attractive for an SHM device.

The key measurement component of the WID systems is the AD5933, an integrated circuit (IC) for impedance measurements. This IC has the ability to measure electrical impedance up to 100 kHz and was chosen because it lowers the total power requirements and chip count of the WID. It has many functions built in that would ordinarily require several additional components, including a signal generator, high-speed analog-to-digital converter (ADC), fast Fourier transform (FFT) analyzer, high-speed digital-to-analog converter (DAC), and anti-aliasing filter.

There are two main options for data storage on the WID 3.0: (1) internal EEPROM that is on the ATmega1281v, and (2) a flash memory module, the Atmel AT26F004. The data storage available in these locations is 8 kB and 500 kB, respectively. This amount is not a vast quantity of storage, but it is sufficient for the type of measurements being made. The measured data are in the frequency domain, and therefore of much smaller size compared to the time series data of other methods. If the data is analyzed before storage, for example with a root mean standard deviation or cross-correlation coefficient, features typically used in impedance methods, and only the analyzed data is stored, the internal EEPROM and flash modules would be able to contain 4000 and 500,000 data points of double precision floating point numbers.

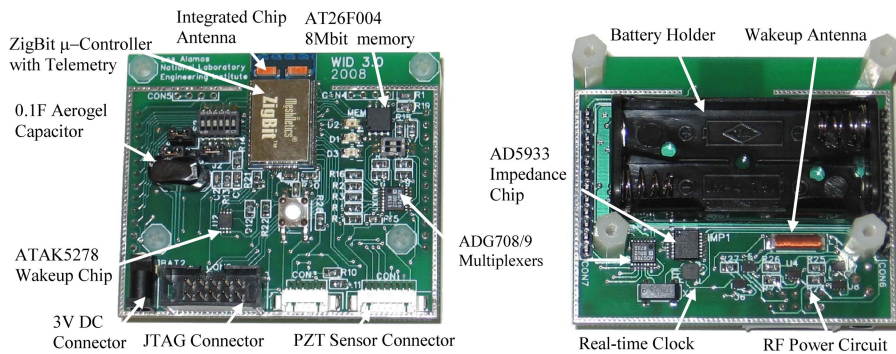


Fig. 2 Major components of the WID3

Table 1 Current draw for the WID 3 components

Component		Current (mA)
Microcontroller	ATmega1281	7
Telemetry chip (3 dBm)	AT86RF230	15.5/16.5 (RX TX)
Impedance chip (active)	AD5933	10
DataFlash (writing)	AT26F004	7
Multiplexer 1	ADG708	0.003
Multiplexer 2	ADG709	0.003
Wake-up chip	ATAK5278	0.09

The previous version of the WID (Mascarenas *et al.* 2007) had the ability to measure only a single sensor, and it also required manual selection of the bypass resistor for range selection. Both of these shortcomings have been addressed with the current WID 3.0 with the addition of two low-power and low-resistance multiplexers, which are shown in Fig. 2. Each multiplexer has eight total inputs, which allows for four resistor ranges and seven sensors to be measured. One of the sensor ports is required for a calibration cycle, which reduces the available sensors from eight to seven.

The WID 3.0 has very low power consumption, especially considering the active nature of its measurements. The WID 3.0 operates at as low as 2.7 V, and it requires 16 seconds to measure four sensors with 100 points and four averages per point. With data reduction, only a few seconds would be required to transmit the data off of the WID to base station, or a few microseconds to store the data on the onboard locations. Initial testing indicates that the current draw could be reduced to approximately 0.01 mA with proper use of sleep modes. At this extremely low power level, the WID could also be powered by a wide range of energy harvesting methods. The current draw of various electronic components is shown in Table 1. The voltage supply for WID3 is designed to provide 2.7 V.

The WID 3.0 can be awakened from sleep states in several ways depending on the capabilities required. The WID3 includes a low frequency (LF) wake-up chip that monitors an inductor low-frequency RF wake-up signal. This monitoring occurs at very low power (0.28 μ W), but at limited range of only 2.5 m. This chip is indicated in Fig. 2, and the inductor coil located above the AD5993 impedance chip. This wake-up capability would be used for on-demand measurements wirelessly triggered by a mobile base station capable of recording the measurements. The second option is an internal timer in the ATmega1281v that can wake the WID3 at intervals on the order of a few seconds to a few weeks. With these solutions available it is conceivable that the WID could run in low-duty cycle operation for decades on a limited power supply. The table below summarizes the power consumption for various modes of operation, and compares these values to those for the

Table 2 Power draw for the WID3 and WID2 in various operation states

Mode	Power (mW)	
	WID3	WID2
Measurement	55	56
Transmit	70.5	61.6
Receive	67.5	N/A
Store	42	N/A

previous version, WID2. It can be seen in the table that the power requirement for WID2 and WID3 are comparable. While the requirement for the WID3 is slightly higher, its increased functionality compensates for its modest increase in power consumption.

2.2 WiDAQ hardware components and capabilities

The capabilities of the WID3 have been further extended to be able to take low frequency measurements from a variety of sensors, such as accelerometers, by combining it with the Wireless Data Acquisition (WiDAQ) board. The combined modular sensor node is shown in Fig. 1 (right). The major components of the WiDAQ are shown in Fig. 3. The WiDAQ is also controlled by an ATmega1281 microcontroller, although it lacks the wireless telemetry capabilities of the WID3. Having its own microcontroller, the WiDAQ can function as a stand-alone device using wired communication, but is primarily intended to be used in combination with the WID3, as shown in Fig. 1 (right). The module connectors, indicated in Figs. 2 and 3, provides each module with the ability to share resources, such as processing power, data storage, and wireless communications. Because each module is equipped with its own microcontroller, both modules need not be awake simultaneously; one module can perform a task and wake the other when it is needed, thereby reducing overall power consumption.

The primary functions of the WiDAQ are data acquisition and signal generation, so the key components on the WiDAQ board are the Analog Devices AD7924 analog-to-digital converter (ADC) chip and the Analog Devices AD5621 digital-to-analog converter (DAC) chip. By excluding sensor-specific conditioning circuitry from the WiDAQ board, sensor data can be acquired from any transducer that provides a voltage output. Sensor-specific conditioning, such as that required for ICP accelerometers, can be included on a third module. The four-channel AD7924 has a 12-bit resolution over a range from zero to 2.5 Volts, and it would consume a maximum of 6 mW while sampling at one million times per second. Because the microcontroller must handle both measurement and telemetry tasks, the full ability of the AD7924 cannot be utilized in the absence of a second dedicated microcontroller. As a result, the effective sampling rate for the WID3 is limited to about 40 kHz, which must be shared among the four channels of the AD7924. With four sensing channels, the effective sampling rate per channel would then be 10 kHz.

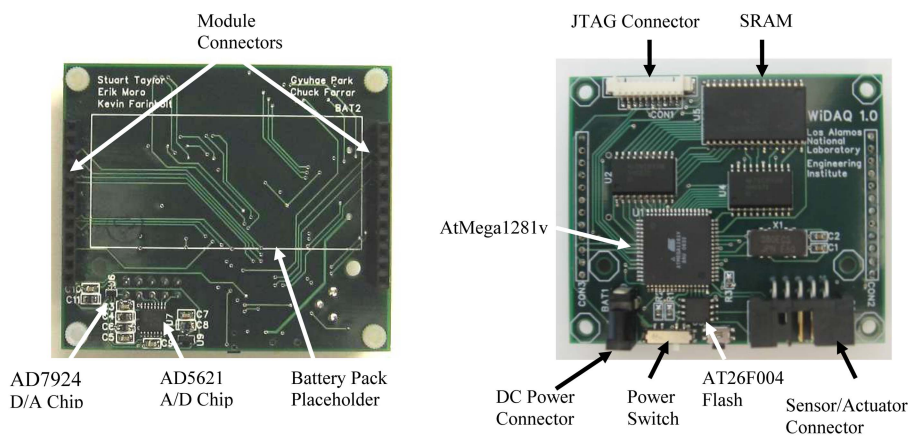


Fig. 3 WiDAQ components



Fig. 4 WiDAQ IPC (left) and assembled modules for vibration data acquisition (right)

The WiDAQ is designed for both passive and active sensing. In addition to the AD7924, an Analog Devices AD5621 D/A converter provides the excitation signal necessary for active sensing using piezoelectric patches. The AD5621 has a 12-bit resolution with an output range of zero to 2.5 Volts, consumes a maximum of 0.5 mW. Each WiDAQ is capable of simultaneously providing an excitation signal through the AD5621 while measuring the response on each of the AD7924's four channels. However, the maximum sampling frequency of 40 kHz must still be shared between the A/D and D/A converters.

Because the WiDAQ does not include any sensor-specific conditioning circuitry, the WiDAQ ICP module has been designed to allow the combined sensor node to function as a complete wireless data acquisition system for ICP accelerometer measurements. The WiDAQ ICP and the complete wireless data acquisition system for ICP accelerometer measurements are pictured in Fig. 4.

3. Impedance measurements for SHM

The experimental verification of the WID for SHM has been reported in the previous papers on monitoring of joint frame structures (Mascarenas *et al.* 2007, 2009), corrosion detection (Overly *et al.* 2008). The performance was also verified in the field test at the Alamosa Canyon Bridge in Southern NM, where we showed that the joints in the bridge could be efficiently monitored with several different WID's operation schemes, including wireless triggering, local networking and wireless energy transmission to power this sensor node (Taylor *et al.* 2009).

4. Sensor diagnostics

This section presents the sensor diagnostic capability of WID3. The WID3 is able to perform sensor diagnostics, where the functionality of sensors/actuators is confirmed to be operational. Validation of the sensor/actuator functionality during SHM operation is a critical component to successfully implement a complete and robust SHM system, especially with an array of PZT active-sensors involved. The basis of this method is to track the capacitive value of PZT transducers, which manifests in the imaginary part of the measured electrical admittance (Park *et al.* 2006a, 2006b). Both degradation of the mechanical/electrical properties of a PZT transducer and the bonding defects between a PZT patch and a host structure can be identified by this process. It is

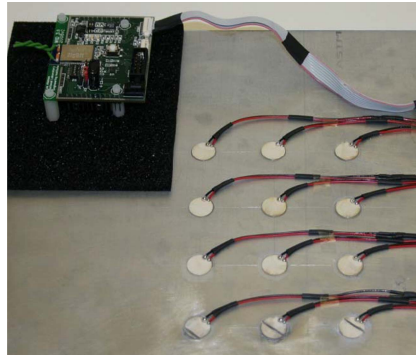


Fig. 5 Sensor diagnostics demonstration plate with healthy, debonded and broken sensors

however found that temperature variations in sensor boundary conditions manifest themselves in similar ways of sensor failures in the measured electrical admittances. Therefore, we have developed an efficient signal processing tool that enables the identification of a sensor validation feature that can be obtained instantaneously without relying on pre-stored baselines and be immune to temperature variations (Overly *et al.* 2009). This diagnostics tools are incorporated in the SHMTools software package, currently under development by the authors. These tools were extended to utilize data collected with the WID3 system.

A sensor diagnostics demonstration plate, shown with the WID3 in Fig. 5, was constructed to test the sensor diagnostics capability. Twelve circular piezoelectric patches are mounted using super-glue on one surface of an Aluminum plate ($30 \times 30 \times 1.25$ cm). The size of the circular PZT patch is 5.5 mm diameter with 0.2 mm thickness. Patches had a different bonding condition, perfect bonding, debonding and sensor breakages. Six patches were under perfect bonding condition, three of them were under the different degree of debonding conditions (25%, 50% and 75% area debonding), and the remaining three were under different fracture conditions (25%, 50% and 75%). To implement the partially bonded samples, a release paper was used to restrict adhesion to only the desired contract regions. Specifically, the PZT patches were bonded to the plate with a corresponding percent of the total area separated by a double layer of release paper. The broken condition was imposed by using a chisel to cut at specific percentages of their total surface area. Admittance measurements in the frequency range of 5-30 kHz were made to each PZT patch after installation

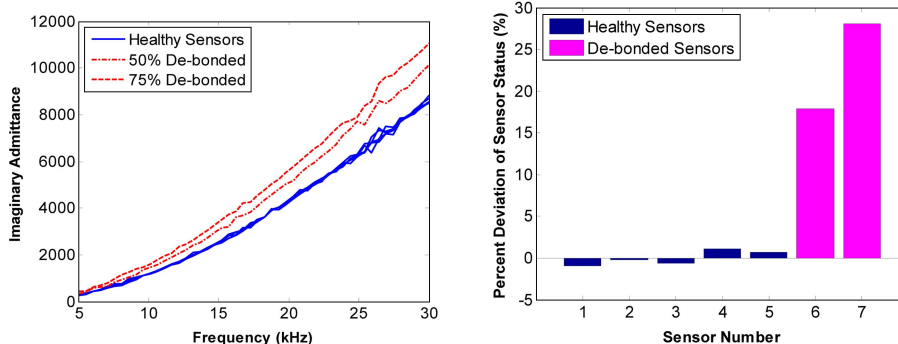


Fig. 6 Raw impedance data collected with the WID3 and auto-classification results from SHMTools for de-bonded sensors

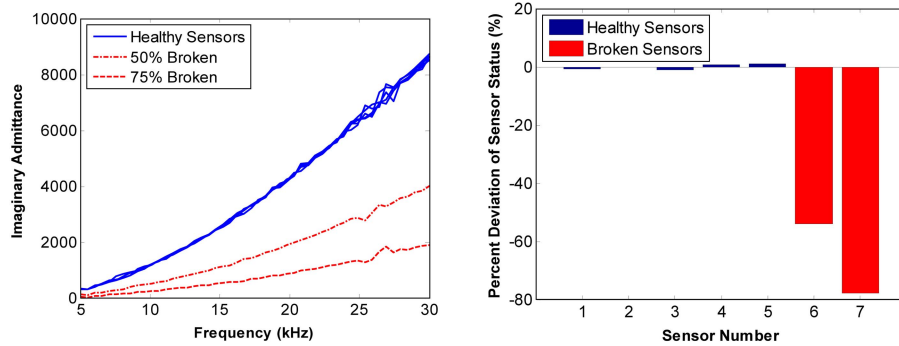


Fig. 7 Raw impedance data collected with the WID3 and auto-classification results from SHMTools for broken sensors

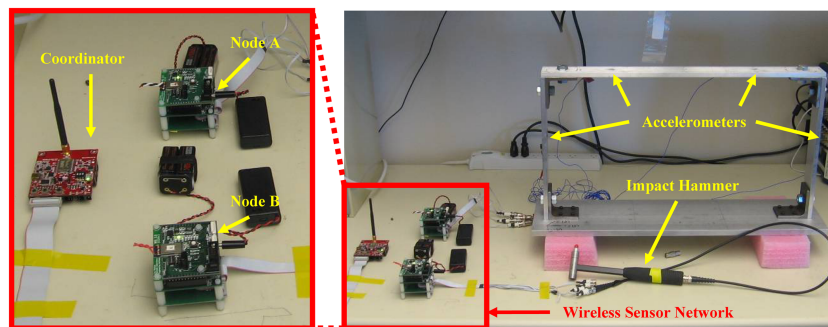


Fig. 8 Laboratory setup for low-frequency vibration test using the WID3/WiDAQ system

using the WID3. The WID3 was powered by two AA batteries for the experiment.

Typical experimental results are illustrated in Figs. 6 and 7. In each scenario, the WID3 is connected to five healthy sensors and two faulty sensors. With induced de-bonding, the slope of the measured admittance is different from the perfect bonding condition (up-ward shifts), and as the de-bonding area increases, there is a corresponding increase in the slope as shown in Fig. 8 (left). At the same time, one can clearly observe in the Fig. 9 that, the slope change (downward shift) of the imaginary admittance is proportional to the breakage percentage. As the breakage percent increases, corresponding decreases in slope were observed. The theoretical basis for this reduction is detailed in the reference (Park *et al.* 2006a). The right side of Figs. 8 and 9 illustrates the results from the SHMTools sensor diagnostics functions using data collected by the WID3. All the sensor conditions were correctly identified with the use of signal processing algorithm developed by the authors, which does not rely on pre-stored baseline measurements. The theoretical basis for the signal processing tools is detailed in the reference (Overly *et al.* 2009). In short, with an array of sensors, this signal processing tool instantaneously identifies a common feature of healthy sensors and applies a process of outlier detection. Sensors with errant bonding or degraded mechanical/electrical properties could be separated by this process. The method is attractive as an array of sensors is typically deployed in active sensing SHM methods. Care does have to be taken to make sure that the sensors being analyzed are exposed to the same environmental conditions and one must use and compare the same size/materials of PZT transducers in order to efficiently use this process and to minimize the variations not related to the sensor conditions (Overly *et al.* 2009).

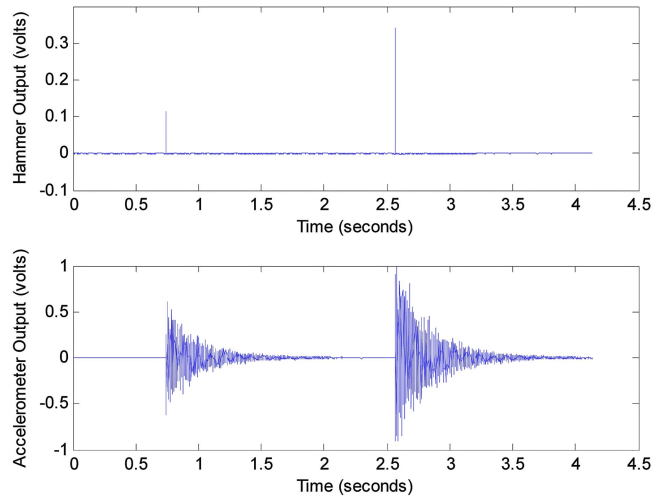


Fig. 9 Time-domain sample record collected using WID3/WiDAQ system

5. Low frequency vibration measurements

This section describes the laboratory testing using the WID3/WiDAQ system to collect time-domain vibrational data for modal analysis. The experimental setup with the sensor node network and test structure is shown in Fig. 8. Two WID3/WiDAQ nodes with ICP conditioning boards were wirelessly networked with a MeshBean board, which served as the network coordinator. In this experiment, the sensor nodes were powered exclusively by batteries. The sensor node network is visible in the figure below (left). Four accelerometers mounted on the test structure were connected to Node A. The accelerometers used were PCB 352A24 “teardrop” accelerometers with a nominal sensitivity of 110 mV/g. An impact hammer was connected to Node B. The impact hammer used was a PCB 086C03, with a nominal sensitivity of 10 mV/lbf.

The wireless network implemented in this experiment utilized a “star” topology, in which the coordinator node communicated directly with each sensor node. Because the modal testing was implemented with a star topology, the command broadcast by the coordinator was received simultaneously by each end device to begin recording. The data could then be handled as digital sequences with identical indices. If the network were more complicated, such as a tiered or mesh network, each device would have to “time-stamp” the recorded data according to a master clock. The accuracy of that clock would then limit the frequency range over which valid measurements could be obtained. The coordinator was connected to a laptop computer using a serial port. At a command from the computer, the coordinator broadcasted an instruction to the two sensor nodes to begin recording sensor data simultaneously. The sensor nodes were preprogrammed to record data at 969 Hz for just over 4 seconds and store the results in the onboard flash memory chips. In this experiment, the measurement parameters were preprogrammed; however, a flexible testing method in which the coordinator also passes commands such as sampling rate and duration could easily be implemented. After storing the data record, each sensor node transmitted its results to the coordinator, which in this case, relayed the data to the laptop computer for later analysis. A sample of the data collected is shown in Fig. 9.

Frequency response functions were estimated using the recorded data, and the test structure’s

Table 3 Comparison of measured natural frequencies using Dactron and WID3/WiDAQ systems

Mode No.	Measured Frequency (Hz)	
	Dactron	WID3/WiDAQ
1	71.42	70.94
2	106.02	105.98
3	185.82	185.68
4	287.26	287.27

Table 4 Comparison of measured natural frequencies using Dactron and WID3/WiDAQ systems

Dactron Auto-MAC		Dactron and WID3/WiDAQ Cross-MAC				WID3/WiDAQ Auto-MAC					
1.00	0.00	0.00	0.19	0.97	0.01	0.00	0.15	1.00	0.00	0.02	0.21
0.00	1.00	0.70	0.00	0.00	0.94	0.68	0.00	0.00	1.00	0.70	0.02
0.00	0.70	1.00	0.00	0.01	0.68	0.98	0.01	0.02	0.70	1.00	0.01
0.19	0.00	0.00	1.00	0.19	0.00	0.00	0.88	0.21	0.02	0.01	1.00

resonant frequencies and mode shapes were extracted using the rational polynomial curve-fitting method (Richardson and Formenti 1982) implemented in DIAMOND, a modal analysis software package developed at Los Alamos National Laboratory (Doebling *et al.* 1997). The extracted resonant frequencies and mode shapes were compared with those obtained using data collected using a 4-channel Dactron™ data acquisition system. The extracted resonant frequencies using each system are shown in Table 3 for the first four modes of vibration. The modal assurance criterion (MAC) was

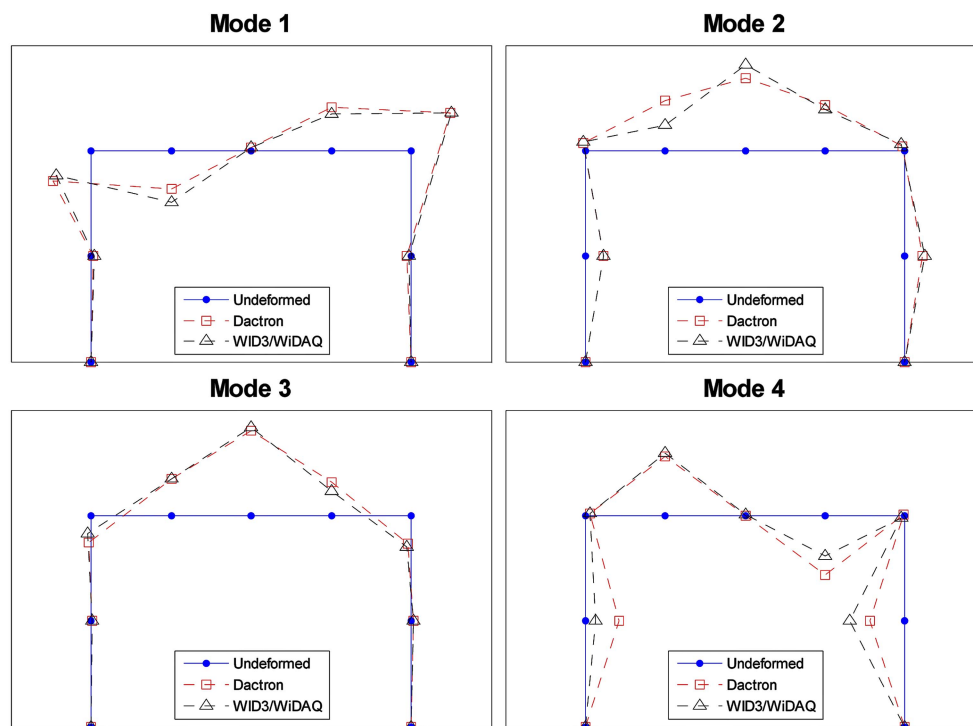


Fig. 10 Line plots of the first four mode shapes obtained using the Dactron and WID3/WiDAQ systems

also computed to compare the mode shapes extracted using the WID3/WiDAQ system with those extracted using the Dactron system. The MAC provides an indication of the degree to which two vectors are aligned; the resulting MAC matrix would be unity on the diagonal for completely correlated vectors, and it would have zeros on the off-diagonals for orthogonal vectors. The auto-MACs for the mode shapes extracted using each system and their cross-MAC are shown in Table 4.

In a controlled laboratory experiment, the correlation between two sets of mode shapes extracted using two different data acquisition systems should be very near unity. For this test, the diagonal MAC values were near unity except for the fourth mode, which had a value of 0.88. Some discrepancies between the mode shapes extracted using the traditional data acquisition system and the WID3/WiDAQ systems, while not significant, can be seen in a line plot of the deformed structure, shown in Fig. 10. These discrepancies could be removed by the use of a higher resolution (such as 16 bit) ADC, but it would require higher power consumption, reducing the effectiveness of the system in areas without access to a constant power supply.

6. Conclusions

Recent developments in the compact wireless impedance device (WID3) have been presented, and the new functionality has been demonstrated. The WID3's most basic capability involves measuring the coupled electromechanical impedance of a structure, capitalizing on the well-established impedance-based structural health monitoring technique to monitor the condition of a structure. The low-power sensor node's capabilities have been extended through improved networking capabilities, increased data storage options, multiple powering options that allow for energy harvesting integration, and increased triggering options that allow for better control of sleep modes, reducing overall power consumption. The capability of this device is demonstrated in structural health monitoring and sensor diagnostic applications. Furthermore, the node's capabilities have been extended through use of a wireless data acquisition (WiDAQ) module to be capable of collecting low-frequency time-domain data from a variety of sensors. To demonstrate this capability, structural vibration data were collected for modal analysis, and the resulting measured natural frequencies and mode shapes were compared to those measured using a traditional data acquisition system. The WID3/WiDAQ serves as a multi-scale sensing module, carrying out an efficient SHM and sensor diagnostic process in high-frequency regimes, as well as monitoring the effects of damage on system-level performance by measuring low-frequency vibration responses. This coupled and multi-scale sensing capability is currently being utilized by the authors for SHM investigations including wind turbine applications, and it will be a subject of subsequent papers.

References

- Bhalla, S. and Soh, C.K. (2004), "Electromechanical impedance modeling for adhesively bonded piezotransducers", *J. Intel. Mat. Syst. Str.*, **15**, 955-972.
- Doebling, S.W., Farrar, C.R. and Cornwell, P.J. (1997), "DIAMOND: a graphical interface toolbox for comparative modal analysis and damage identification", *Proceedings of the 6th International Conference on Recent Advances in Structural Dynamics*, Southampton, UK.
- Giurgiutiu, V., Zagari, A. and Bao, J.J. (2004), "Damage identification in aging aircraft structures with piezoelectric wafer active sensors", *J. Intel. Mat. Syst. Str.*, **15**, 673-688.

- Grisso, B.L. and Inman, D.J. (2008), "Autonomous hardware development for impedance-based structural health monitoring", *Smart Struct. Syst.*, **4**(3), 305-318.
- Kim, J.K., Zhou, D., Ha, D.S. and Inman, D.J. (2009), "A practical system approach for fully autonomous multi-dimensional structural health monitoring", *Proceedings of SPIE's 16th Annual Smart Structures and Materials Conference*, San Diego, CA, March.
- Kim, J.T., Park, J.H., Hong, D.S. and Park, W.S. (2010), "Hybrid health monitoring of prestressed concrete girder bridges by sequential vibration-impedance approaches", *Eng. Struct.*, **32**(1), 115-128.
- Lynch, J.P. and Loh, K.J. (2006), "A summary review of wireless sensors and sensor networks for structural health monitoring", *Shock Vib. Digest*, **38**(2), 91-128.
- Mascarenas, D., Todd, M.D., Park, G. and Farrar, C.R. (2006) "Remote inspection of bolted joints using RFID-tagged piezoelectric sensors", *Proceedings of 24th International Modal Analysis Conference*, St. Louis, MO, January- February.
- Mascarenas, D.L., Todd, M.D., Park, G. and Farrar, C.R. (2007), "Development of an impedance-based wireless sensor node for structural health monitoring", *Smart Mater. Struct.*, **16**(6), 2137-2145.
- Mascarenas, D.L., Park, G., Farinholt, K.M., Todd, M.D. and Farrar, C.R. (2009), "A low-power wireless sensing device for remote inspection of bolted joints", *Proceedings of the Institution of Mechanical Engineers, Part G: Journal of Aerospace Engineering*, **233**(5), 565-575.
- Overly, T.G., Park, G., Farinholt, K.M. and Farrar, C.R. (2008), "Development of an extremely compact impedance-based wireless sensing device", *Smart Mater. Struct.*, **17**(6).
- Overly, T.G., Park, G., Farinholt, K.M. and Farrar, C.R. (2009), "Piezoelectric active-sensor diagnostics and validation using instantaneous baseline data", *IEEE Sens. J.*, **9**(11), 1414-1421.
- Park, G., Sohn, H., Farrar, C.R. and Inman, D.J. (2003), "Overview of piezoelectric impedance-based health monitoring and path forward", *Shock Vib. Digest*, **35**, 451-463.
- Park, G., Farrar, C.R., Rutherford, A.C. and Robertson, A.N. (2006a), "Piezoelectric active sensor self-diagnostics using electrical admittance measurements", *J. Vib. Acoust.*, **128**, 469-476.
- Park, G., Farrar, C.R., Lanza di Scalea, F. and Coccia, S. (2006b) "Performance assessment and validation of piezoelectric active sensors in structural health monitoring", *Smart Mater. Struct.*, **15**(6), 1673-1683.
- Park, S., Ahmad, S., Yun, C.B. and Roh, Y. (2006c), "Multiple crack detection of concrete structures using impedance-based structural health monitoring technique", *Exp. Mech.*, **46**, 609-618.
- Park, S., Shin, H.H. and Yun, C.B. (2009a), "Wireless impedance sensor nodes for functions of structural damage identification and sensor self-diagnostics", *Smart Mater. Struct.*, **18**(5).
- Park, S., Park, G., Yun, C.B. and Farrar, C.R. (2009b), "Sensor self-diagnosis using a modified impedance model for active-sensing structural health monitoring", *Struct. Health Monit.*, **8**(1), 71-82.
- Richardson, M.H. and Formenti, D.L. (1982), "Parameter estimation from frequency response measurements using rational fraction polynomials", *Proceedings of the 1st International Modal Analysis Conference*, Orlando, FL.
- Spencer, B.F., Ruiz-Sandoval, M.E. and Kurata, N. (2004), "Smart sensing technology: opportunities and challenges", *Struct. Control Health Monit.*, **11**(4), 349-368.
- Taylor, S.G., Farinholt, K.M., Flynn, E.B., Figueiredo, E., Mascarenas, D.L., Park, G., Todd, M.D. and Farrar, C.R. (2009), "A mobile-agent based wireless sensing network for structural monitoring applications", *Meas. Sci. Technol.*, **20**(4).
- Wang, S. and You, C. (2008), "A circuit design for impedance-based structural health monitoring", *J. Intel. Mat. Syst. Str.*, **19**(9), 1029-1040.
- Worden, K. and Dulieu-Barton, J.M. (2004), "An overview of intelligent fault detection in systems and structures", *Struct. Health Monit.*, **3**(1), 85-98.
- Zhou, D., Kim, J.K., Bile, J.L., Shebi, A., Ha, D.S. and Inman, D.J. (2009), "Ultra low-power autonomous wireless structural health monitoring node", *Proceedings of the 7th International Workshop on Structural Health Monitoring*, Palo Alto, CA, September.